Available online at www.sciencedirect.com
ScienceDirect
Journal of the European Ceramic Society 28 (2008) 2319–2324
www.elsevier.com/locate/jeurceramsoc

Residual stresses in YAG phase in directionally solidified eutectic Al_2O_3/YAG ceramic composite estimated by X-ray diffraction

J.J. Sha [a,*], S. Ochiai [a], H. Okuda [a], Y. Waku [b], N. Nakagawa [b], A. Mitani [b], M. Sato [b], T. Ishikawa [b]

[a] *International Innovation Center, Kyoto University, Sakyo-ku 606-8501, Japan*
[b] *Ube Industries Ltd., Ube, Yamaguchi 755-8633, Japan*

Available online 4 March 2008

Abstract

The residual stresses in YAG phase in directionally solidified eutectic (DSE) $Al_2O_3/Y_3Al_5O_{12}$ (YAG) ceramic composite were estimated by X-ray diffraction technique. The YAG skeleton specimen without Al_2O_3 phase, extracted from the composite, was used as a thermally-induced stress-free reference specimen. The X-ray stress measurements with Cu Kα irradiation were performed on the two planes: parallel and perpendicular to the solidification direction. The estimated residual stresses on average were −220 MPa and −157 MPa on the planes parallel and perpendicular to the solidification direction, respectively. The measured residual stresses were described fairly well by the calculation based on a lamellar model under the condition of the stress-free temperature 1400–1600 K.

Keywords: Eutectic composite; Residual stresses; X-ray diffraction

1. Introduction

Because of the attractiveness in superior oxidation resistance, high stability of the microstructure and excellent high temperature mechanical properties in oxidative environment, directionally solidified eutectic (DSE) oxide/oxide ceramic composites are potential structural materials for advanced energy generation systems and propulsion systems.[1,2] Recently, a number of DSE oxide/oxide ceramic composites, such as $Al_2O_3/Y_3Al_5O_{12}$,[3–5] Al_2O_3/ZrO_2,[6] $Co_{1-x}Ni_x/ZrO_2(CaO)$,[7] and $Al_2O_3/GdAlO_3$,[8] have been developed, being expected to fulfill the requirements for ultra high temperature applications.

Since DSE ceramic composites are generally fabricated and are to be used in an ultra high temperature environment, one of the key issues is to reveal the residual stresses, arising from the mismatch of coefficient of thermal expansion (CTE) among the constituting phases on cooling from the fabrication and application temperatures. To ensure these composites operate safely as high temperature structural components, the residual stress should be taken into consideration in engineering design and real application, because such residual stress (compressive in one phase and tensile in the other) will certainly have an affect on the mechanical behavior of these composites.[8,9] Therefore, an understanding of the residual stress state in DSE ceramic composites is essential for engineering application.

Among the DSE ceramic composites mentioned above, the Al_2O_3/YAG (Yttrium–Aluminum Garnet with the composition of $Y_3Al_5O_{12}$) ceramic composite is a very promising candidate for high temperature structural components due to the good thermal expansion compatibility between the Al_2O_3 and YAG phases,[10,11] clean interface between the phases without glass phase, and high mechanical properties and high stability in ultra high temperature region.[3–5,12] The next step for application is to clarify the residual stress. The accurate estimation of the thermal residual stresses is, however, a complex problem, because the microstructure and crystallographic texture of DSE ceramic composites are very sensitive to processing conditions as have been reported[13–15] and therefore the thermal residual stresses depend not only on the CTE mismatch but also on the cooling rate, the morphology of the eutectic microstructure, and the stress relaxation mechanism.

The three-dimensional observation of the eutectic structure and the crystallographic orientation relationships between the two eutectic phases in DSE Al_2O_3/YAG ceramic composite have been characterized by Yasuda et al. by means of X-ray tomography analysis.[16] In the current work, the YAG skeleton specimen

* Corresponding author. Tel.: +81 75 753 5194; fax: +81 75 753 4841.
E-mail address: shajianjun@iic.kyoto-u.ac.jp (J.J. Sha).

0955-2219/$ – see front matter © 2008 Elsevier Ltd. All rights reserved.
doi:10.1016/j.jeurceramsoc.2008.01.018

without Al_2O_3 phase, extracted from the composite, was used as a thermally-induced stress-free reference specimen, and the residual stresses in YAG phase in the composite on the planes parallel and perpendicular to the solidification direction, were estimated by the X-ray diffraction technique. Then, the residual stresses estimated by the X-ray measurements were compared with those predicted by the lamellar model as a first approximation to know the influence of the stress-free temperature on the residual stress-values.

2. Materials and experimental procedure

2.1. Specimen

The DSE Al_2O_3/YAG ceramic composites were fabricated by a Bridgman method at the Ultra-high Temperature Materials Research Center, Yamaguchi, Japan. The fabrication procedure has been described in detail elsewhere.[3-5] The surface morphologies of the fabricated specimen are shown in Fig. 1. The alumina and YAG phases correspond to the dark and light phases, respectively.

In the fabricated specimens, the volume fraction of Al_2O_3 and YAG are the same (50%).[3,4] The widths of alumina and YAG phases are around 10–30 μm. The single crystal Al_2O_3 and YAG phases are three-dimensionally continuous and entangled.[16] The alumina and YAG crystals on the plane parallel to the solidification are elongated in comparison with those on the plane perpendicular to it.

The specimen's dimension was 10 mm (length) × 10 mm (width) × 10 mm (thickness). For distinguishing the surfaces in the X-ray stress measurement, based on the crystallographic orientation of Al_2O_3 phase in the composite, the mutually perpendicular surfaces in the specimen shown in Fig. 1, were assigned *a*, *b*, and *c*. Correspondingly, each surface was defined as *a*, *b*, and *c* direction. The solidification is along the *b* direction (Fig. 1).

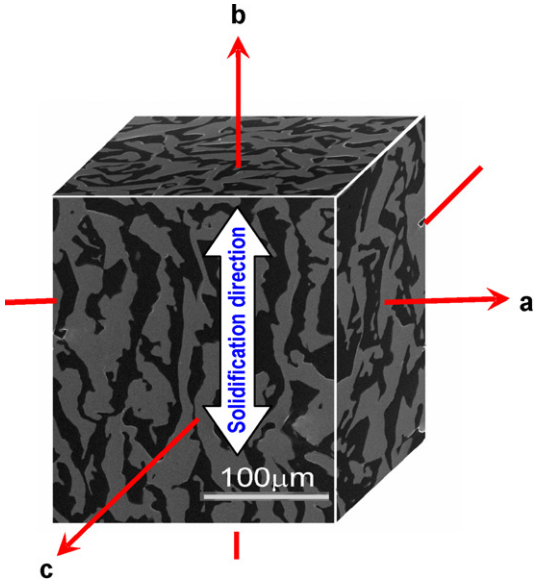

Fig. 1. Surface morphologies of DSE Al_2O_3/YAG ceramic composite, the dark phase and light phase in this composite correspond to the Al_2O_3 and the YAG phases.

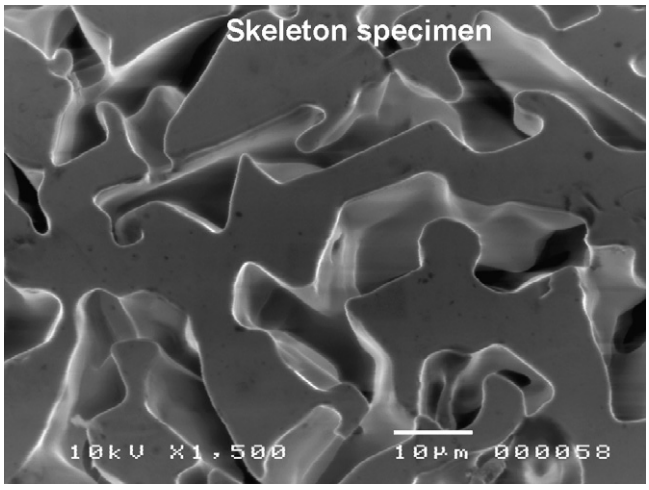

Fig. 2. The surface morphology of skeleton specimen showing a porous microstructure.

In order to measure the unstressed lattice parameter, d_0, the sheets with a dimension of 10 mm (length) × 10 mm (width) × 0.6 mm (thickness) were prepared, from which the Al_2O_3 phase was removed by a treatment to make them fully porous on a surface layer[8] and the skeleton YAG specimen was obtained. The surface morphologies of the skeleton specimen are shown in Fig. 2. The skeleton YAG specimen without alumina phase was used as the reference (unstressed specimen) for X-ray strain measurement. The use of skeleton YAG specimen minimized the composition fluctuation and microstructure difference in comparison with those of the as-received specimen.

2.2. X-ray diffraction

The X-ray diffraction method for the measurement of stresses in crystalline solids has been well established.[17,18] In this method, the interplanar spacing *d* is used as an absolute strain gauge. The interplanar spacing, *d*, for a particular set of *h k l* planes of a given phase can be measured from the corresponding peak in the diffraction pattern with Bragg's law:

$$d = \frac{\lambda}{2 \sin \theta_B} \quad (1)$$

where θ_B is the Bragg angle, which was obtained from the measurement of Kα1 peak position in the present work. XRD patterns were measured by a Rigaku X-ray diffractometer (RINT 2000 series, Model D/max-2200) with a four-circle goniometer (φ, ψ, ω, 2θ which will be defined below).

The X-ray diffraction setup and specimen mounting are shown in Fig. 3. The specimen can rotate in its own plane about an axis (A–A′) normal to its surface, and about a horizontal axis (B–B′) as shown in Fig. 3. The horizontal axis lies in the specimen surface and it is initially adjusted by rotation about the diffractometer axis (perpendicular to the drawing), to make equal angles with the incidence and diffraction beams.

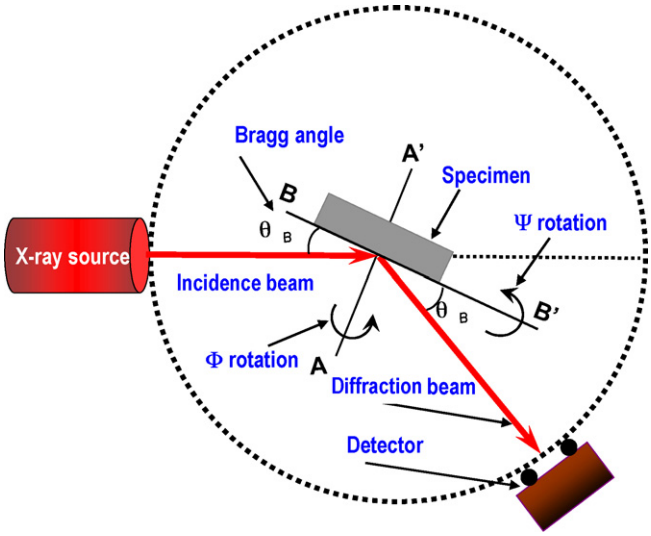

Fig. 3. The X-ray diffraction setup and specimen mounting, and definition of rotation axes for both ϕ and ψ angles.

After such an adjustment, the horizontal axis is fixed (no further rotation about the diffractometer axis).

In order to know the residual stress states in this composite, two coordinate systems, the laboratory coordinate system and specimen coordinate system, were defined. Fig. 4 shows a laboratory coordinate system X_i^L with respect to a specimen coordinate system X_i^S and the definition of ψ and φ angles. The direction of the incident beam with respect to the specimen's coordinates was determined by these two angles: ψ and φ (see Figs. 3 and 4). The specimen was mounted onto a goniometer head that was used to position a specimen in the X-ray beam and was oriented with respect to the specimen coordinate system (X_i^S) so that the φ axis coincided with the normal (X_3^S) of the surface of the specimen throughout the experiment (Fig. 4). In this work, the X_1^S direction was chosen as the reference for angle φ. In the drawing of Fig. 3, the ψ angle is zero when the surface of specimen is vertical and has value of 90° when the surface of specimen is in the horizontal position. Both angles ψ and φ were taken from the pole figure analysis.

During the X-ray stress measurement, a Cu Kα irradiation was used at 40 kV and 200 mA. The relevant diffractometer conditions are summarized in Table 1. The direction of strain

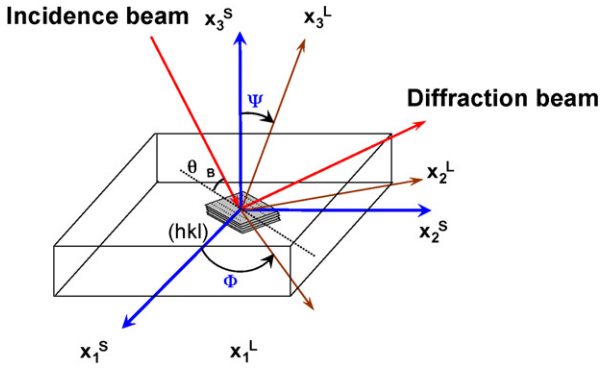

Fig. 4. Establishment of the laboratory coordinate system and the specimen coordinate system, and the definition of ϕ and ψ angles in the present specimen.

Table 1
X-ray diffractometer conditions for residual strain measurement

Parameter	Condition
Equipment	Rigaku XRD: Cu Kα X-ray tube; four circle goniometer
Power	8 kW; 40 kV, 200 mA
Radiation	Cu Kα, λ = 1.540562 Å
Diffraction	{8 8 8}
2θ range	125.1–125.8°
Divergence slit	0.25°; 2.0 mm horizontal window
Soller slit	0.25°
Receiving slit	0.15 mm
Source-to-specimen distance	185 mm
Scans	Step: 0.004°; 2θ/step; 2.4 s/step

measurement with respect to the specimen was always along the bisector of the incident and diffracted beams, namely, along the X_3^L axis normal to the diffraction planes (Fig. 4).

Generally, the diffraction peak in the high 2θ region is chosen for residual stress measurement because a high-angle peak will result in a larger shift in 2θ for a given stress. In the present work, the 8 8 8 plane (peak position at 2θ = 125.386°) for YAG phase was chosen for strain measurement, and the X-ray strain measurements were performed on the two planes: parallel (*c* plane) and perpendicular (*b* plane) to the solidification direction (*b* axis) (Fig. 1).

Before the X-ray strain measurements, the pole figure analysis was performed to determine the orientation of each member of the YAG 888 family of diffractions using the Shultz reflection method.[18] The orientation for each diffraction member was determined by angles ϕ and ψ. By rotating the goniometer by a combination of ϕ and ψ degrees, a particular diffraction normal was brought into the diffraction plane. Then a 2θ/θ scan was collected from each accessible member of the YAG 888 family of diffractions.

3. Results

The peak profiles for both as-received and skeleton specimens were obtained in the range of 125.1–125.8° for YAG 888 diffractions. Examples (dot curve) in Fig. 5 show Gaussian distribution in intensities. Evidently, the peak profile in the as-received specimen is broadened and shifted to higher 2θ in comparison with that of the skeleton specimen. The shift and broadening of the peak observed in the as-received specimen implies the existence of elastic residual stresses and their inhomogeneous distribution. To obtain the diffracted peak positions precisely, the 2θ positions were determined by fit of the background-subtracted peaks to the Gaussian function (only the data with intensities higher than 70% of maximum intensity was used). Examples of the fitting profiles (solid curve) are shown in Fig. 5.

The strain, $e_{hkl}^{\phi\psi}$, can be obtained from different crystallographic planes ($d_{hkl}^{\phi\psi}$) and the unstressed lattice parameter (d_0) by the following equation:

$$e_{hkl}^{\phi\psi} = \frac{d_{hkl}^{\phi\psi} - d_0}{d_0} \quad (2)$$

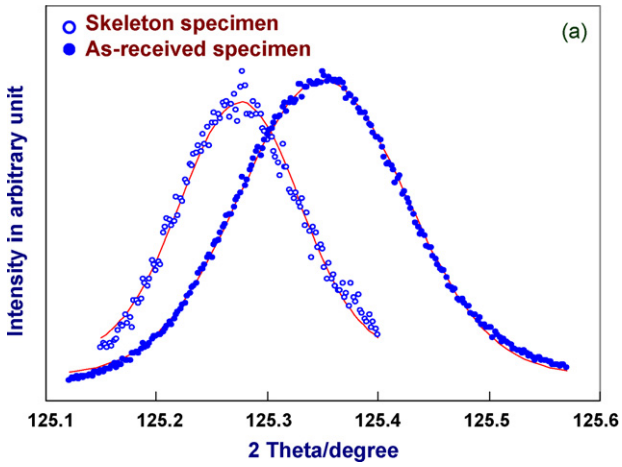

Fig. 5. Peak profiles measured from YAG 888 family of diffractions and fitting lines for as-received and skeleton specimen.

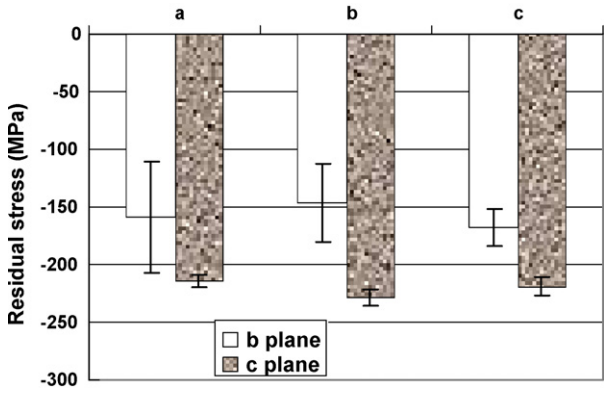

Fig. 6. The principal residual stresses measured from YAG 888 family of diffractions on both *b* and *c* planes.

where $e_{hkl}^{\phi\psi}$ is the measured strain for diffraction $(h\,k\,l)$ located at φ and ψ (along the X_3^{L} direction).

Using the relationship between the two coordinate systems, the strain tensor ε_{ij} in the specimen coordinate system (X_i^{S}) can be expressed by the following equation:

$$e_{hkl}^{\phi\psi} = a_i a_j \varepsilon_{ij} \tag{3}$$

where a_i is the direction cosine between the $(h\,k\,l)$ diffraction and axis i. The strain tensors in the specimen coordinate system can be determined with generalized least-square method.[19] In the present experiments, less than six diffractions for YAG 888 family were identified on pole figure, only the principal strains (normal to each surface of specimen) were measured.

The residual stress tensor σ_{ij} in YAG phase was calculated from the measured strains using the relation:[18]

$$\varepsilon_{ij} = \frac{1+\nu}{E}\sigma_{ij} - \delta_{ij}\frac{\nu}{E}\sigma_{kk} \tag{4}$$

Here $\delta_{ij} = 1$ for $i = j$, and $\delta_{ij} = 0$ for $i \neq j$, and ν and E are Poisson's ratio and Young's modulus of materials, respectively. The Young's modulus and Poisson's ratio of the YAG phase were taken to be 294 GPa, and 0.25, respectively.[20] The errors in the measured stresses were obtained from those of strains using the method in a previous study.[19] Fig. 6 shows the measured residual stresses and error bars for *b* and *c* planes. The average principal residual stresses in the YAG phase were −220 MPa and −157 MPa on the planes parallel and perpendicular to the solidification direction, respectively.

4. Discussion

The results in Fig. 6 indicated that the principal residual stresses in YAG phase varied with varying direction and measured planes. The average values of principal residual stresses in YAG phase were −220 MPa and −157 MPa on the *c* plane and *b* plane, respectively. These results may be associated with the anisotropic properties and local microstructure heterogeneity of constitute phases. For single crystal alumina phase, an anisotropic CTE has been observed in the basal plane and *c* axis, and the CTE is higher in *c* axis in comparison with those of other axis.[21] This could be a reason for the relatively high residual stress measured on the *c* plane. In addition, the Cu Kα irradiation used in the X-ray strain measurement has a penetration depth of about 125 μm (for 90% attenuation) obtained from the method in the literature.[17] Thus, the X-ray penetration depth was large compared with the phase dimensions (10–30 μm). The residual stress in the present study is an average value of about 125 μm thickness from the measured surface and it can be affected by the morphologies of eutectic phases in the X-ray irradiated volume. On the other hand, the accuracy of residual stresses may be affected by the measurement of the unstressed lattice parameter. Small variations in d_0 can greatly affect on the accuracy of the strain measurement, especially, for DSE Al_2O_3/YAG ceramic composite with small CTE mismatch. In previous study,[22,23] the measured residual stresses by X-ray diffraction are nearly zero within the experimental error. However, in the present study, the d_0 was measured from the skeleton YAG specimen. The advantage by using the skeleton specimen has been described in Section 2.1. In addition, during the preparation of skeleton specimen, the high temperature annealing would be helpful in the relaxation of residual stress.

As shown in Fig. 1, the alumina and YAG crystals on the plane parallel to the direction of solidification are elongated. For rough prediction of the thermal mismatch stresses and for understanding the mechanism for residual stresses development, the model[24] for DSE ceramic composite with a lamellar microstructure was applied in the present work as a first approximation, as follows. In this model, the thermal residual stresses are generated on cooling in YAG phase as schematically illustrated in Fig. 7. It is noted that it has been shown by Yoshida et al.[25] that the flow stress of this composite under applied stress parallel to the solidification direction at high temperatures (>1600 K) can be described well by such a lamellar model. This result suggests that the present model could also be used for description of the residual stress for the direction parallel to the solidification as a rough approximation.

As a first approximation, the lamellar microstructure of the DSE ceramic composites was regarded to be fully constrained, isotropic, elastic slabs. Under such an approximation, the

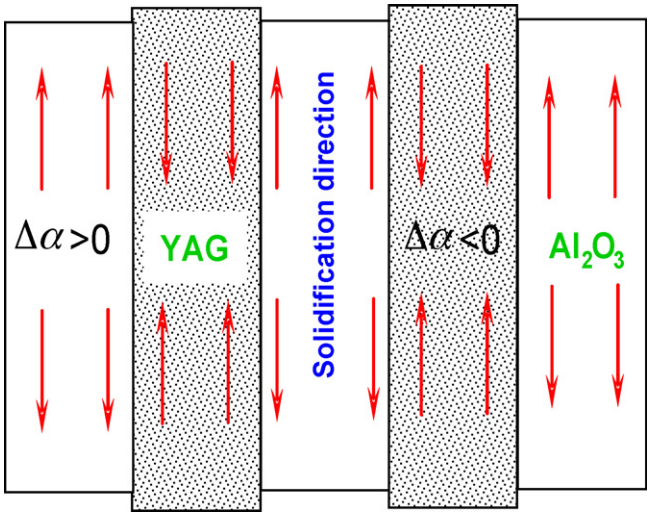

Fig. 7. Schematic illustration of lamellar structure showing the presence of residual stresses with arrows.

in-plane thermal mismatch stresses can be calculated as:[24]

$$\sigma^{\mathrm{Y}} = \int_{T_{\mathrm{room}}}^{T_{\mathrm{stress}}} \Delta\alpha(T)\frac{E^{\mathrm{Y}}(T)}{1-\nu^{\mathrm{Y}}} \left[1+\left(\frac{t^{\mathrm{Y}}}{t^{\mathrm{A}}}\right)\left(\frac{E^{\mathrm{Y}}(T)/(1-\nu^{\mathrm{Y}})}{E^{\mathrm{A}}(T)/(1-\nu^{\mathrm{A}})}\right)\right]^{-1} \mathrm{d}T \quad (5)$$

where σ^{Y} is the residual stress of phase YAG on the plane paralleled to the interface, $\Delta\alpha(T)\,\mathrm{d}T$ is the thermal mismatch strain between the two eutectic phases, E^{i} and ν^{i} are Young's modulus and Poisson's ratio of phase i (i = A for alumina and i = Y for YAG), respectively, and t^{i} is the thickness of layer i. In this model, the temperature dependence of CTE and Young's modulus was taken from our previous work:[20] $E^{\mathrm{Y}} = 299 - 0.0180T$ (GPa), $E^{\mathrm{A}} = 423 - 0.0474T$ (GPa), $\alpha^{\mathrm{Y}} = 6.09 + 0.00117T$ ($\times 10^{-6}$/K), $\alpha^{\mathrm{A}} = 6.50 + 0.00146T$ ($\times 10^{-6}$/K). The Poisson's ratios are 0.23 for Al_2O_3 phase and 0.25 for YAG phase, respectively. Since the CTE of the YAG phase is less than that of the alumina phase, the alumina shrinks more than YAG on cooling, but the YAG resists it. Such an interaction puts the YAG phase in compression and the alumina in tension as indicated by arrow in Fig. 7.

In order to estimate the thermal residual stresses with Eq. (5), it is necessary to know the stress-free temperature,[21] above which the residual stress is released due to the creep/plastic deformation of alumina and below which the residual stress is accumulated. Such a temperature is considered to be dependent on the cooling rate since the high temperature deformation of alumina is time-dependent.[26] In the present work, various stress-free temperatures in the range from 1400 K (around onset temperature of deformation of alumina[21]) and 2200 K (melting point of the composite) were assumed. The calculation results are presented in Fig. 8, in which the residual stress at room temperature in the longitudinal direction in Fig. 7 is plotted against the stress-free temperature. From the result in Fig. 8, it can be seen that the residual stress is highly dependent on the stress-free temperature.

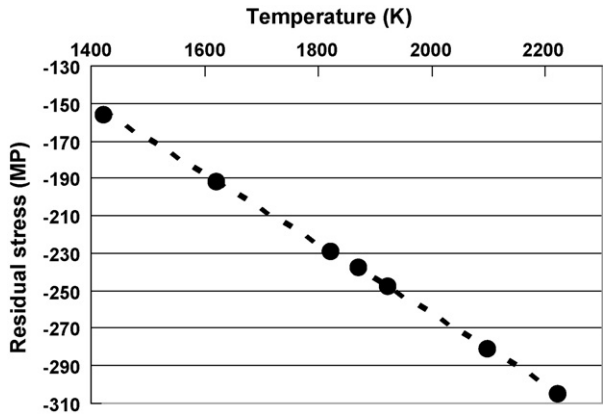

Fig. 8. The thermal mismatch residual stresses estimated by Eq. (5) and their dependence on the stress-free temperature at which the plastic deformation occurred.

Comparing the stresses from experiment with those from model's prediction, the X-ray measured residual stresses is very similar to those of model predictions in the low temperature region (1400–1600 K). This is parallel with the minimum temperature, which is at 1423 K in prismatic and pyramidal planes,[21] for the activation of plastic deformation in single crystal aluminum phase. Meanwhile, this result indicates that X-ray diffraction technique used in present work is appropriate and revealed that the elastic residual stresses are unnecessarily generated at eutectic temperature.

Although the used model is simple in estimation of residual stress in DSE ceramic composites, it can give some instructive information and predict the stress magnitude. It is noted that a more refined model based on the real microstructure by finite element method (FEM) under the condition of the stress-free temperature 1423 K revealed that the average residual stress in the direction parallel to the solidification was −180 MPa on an average,[27] with which the present result is consistent.

5. Conclusion

The residual stresses in YAG phase of directionally solidified eutectic $Al_2O_3/Y_3Al_5O_{12}$ (YAG) ceramic composite were estimated by X-ray diffraction technique. It was found that the average residual stresses are −220 MPa and −157 MPa on the planes parallel and perpendicular to the solidification direction, respectively. The measured residual stresses were similar to those calculated by a lamellar model for the stress-free temperature 1400–1600 K.

Acknowledgement

The financial support from the Japan Society for the Promotion of Science (JSPS) is gratefully acknowledged.

References

1. Hirano, K., Application of eutectic composites to gas turbine system and fundamental fracture properties up to 1700 °C. *J. Eur. Ceram. Soc.*, 2005, **25**, 1191–1199.

2. Nakagawa, N., Ohtsubo, H., Mitani, A., Shimizu, K. and Waku, Y., High temperature strength and thermal stability for melt growth composite. *J. Eur. Ceram. Soc.*, 2005, **25**, 1251–1257.
3. Waku, Y., Otsubo, H., Nakagawa, N. and Kohtoku, Y., Sapphire matrix composites reinforced with single crystal YAG phases. *J. Mater. Sci.*, 1996, **31**, 4663–4670.
4. Waku, Y., Nakagawa, N., Wakamoto, T., Otsubo, H., Shimizu, K. and Kohtoku, Y., High temperature strength and thermal stability of unidirectionally solidified Al_2O_3/YAG eutectic composite. *J. Mater. Sci.*, 1998, **33**, 1217–1225.
5. Waku, Y., Nakagawa, N., Wakamoto, T., Shimizu, K. and Kohtoku, Y., The creep and thermal stability characteristics of a unidirectionally solidified Al_2O_3/YAG eutectic composite. *J. Mater. Sci.*, 1998, **33**, 4943–4951.
6. Homeny, J. and Nick, J. J., Microstructure property relations of alumina zirconia eutectic ceramics. *Mater. Sci. Eng. A*, 1990, **127**, 123–133.
7. Brewer, L. N., Dravid, V. P., Dhalenne, G. and Velazquez, M., Solid solution directionally solidified eutectic oxide composites: I. Eutectic growth and characterization. *J. Mater. Res.*, 2002, **17**, 760–767.
8. Waku, Y., Nakagawa, N., Wakamoto, T., Ohtsubo, H., Shimizu, K. and Kohtoku, Y., A ductile ceramic eutectic composite with high strength at 1873 K. *Nature (London)*, 1997, **389**, 49–52.
9. Kinlich, A. L., Thrusabanjong, E. and Williams, L. G., Fracture at biomaterial interfaces: the role of residual stresses. *J. Mater. Sci.*, 1991, **26**, 6260–6270.
10. Touloukian, Y. S., *Thermophysical Properties of High Temperature Solid Materials, Vol. 4, Oxides and Their Solutions and Mixtures*. Macmillan, New York, 1967.
11. Gupta, T. K. and Valentich, J., Thermal expansion of yttrium aluminum garnet. *J. Am. Ceram. Soc.*, 1971, **54**, 355–356.
12. Ochiai, S., Sakai, Y., Sato, K., Tanaka, M., Hojo, M., Okuda, H. *et al.*, Fracture characteristics of Al_2O_3/YAG composite at room temperature to 2023 K. *J. Eur. Ceram. Soc.*, 2005, **25**, 1241–1249.
13. Matson, L. E. and Hecht, N., Microstructural stability and mechanical properties of directionally solidified alumina/YAG eutectic monofilaments. *J. Eur. Ceram. Soc.*, 1999, **19**, 2487–2501.
14. Farmer, S. C. and Sayir, A., Tensile strength and microstructure of Al_2O_3–ZrO_2 hypo-eutectic fibers. *Eng. Fracture Mech.*, 2002, **69**, 1015–1024.
15. Sayir, A. and Farmer, S. C., The effect of the microstructure on mechanical properties of directionally solidified Al_2O_3/ZrO_2(Y_2O_3) eutectic. *Acta Mater.*, 2000, **48**, 4691–4697.
16. Yasuda, H., Ohnaka, I., Mizutani, Y., Morikawa, T., Takeshima, S., Sugiyama, A. *et al.*, Three-dimensional observation of the entangled eutectic structure in the Al_2O_3-YAG system. *J. Euro. Ceram. Soc.*, 2005, **25**, 1397–1403.
17. Cullity, B. D., *Elements of X-ray Diffraction* (*2nd ed.*). Addison Wesley, Reading, MA, 1978, p. 292.
18. Noyan, I. C. and Cohen, J. B., *Residual Stress: Measurement by Diffraction and Interpretation*. Springer-Verlag, New York, 1987, pp. 117–162.
19. Winholtz, R. A. and Cohen, J. B., Generalized least-squares determination of triaxial stress states by X-ray diffraction and the associated errors. *Aust. J. Phys.*, 1988, **41**, 189–199.
20. Ochiai, S., Ueda, T., Sato, K., Hojo, M., Waku, Y. and Sakata, S., Elastic modulus and coefficient of thermal expansion of Al_2O_3/YAG composite at room to ultra high temperatures. *Mater. Sci. Res. Int. Special Tech. Publ.*, 2001, **2**, 281–285.
21. LLorca, J. and Orera, V. M., Directionally solidified eutectic ceramic oxides. *Prog. Mater. Sci.*, 2006, **51**, 711–809.
22. Dickey, E. C., Frazer, C. S., Watkins, T. R. and Hubbard, C. R., Residual stresses in high temperature ceramic eutectics. *J. Eur. Ceram. Soc.*, 1999, **19**, 2503–2509.
23. Ashbrook, R. L., Directionally solidified ceramic eutectics. *J. Am. Ceram. Soc.*, 1997, **60**, 428–435.
24. Hillman, C., Suo, Z. and Lange, F. F., Cracking of laminates subjected to biaxial tensile stresses. *J. Am. Ceram. Soc.*, 1996, **79**, 2127–2133.
25. Yoshida, H., Nakamura, A., Sakuma, T., Nakagawa, N. and Waku, Y., Anisotropy in high-temperature deformation in unidirectionally solidified eutectic Al_2O_3-YAG single crystals. *Scripta Mater.*, 2001, **45**, 957–963.
26. Kim, H. S. and Roberts, S., Brittle-ductile transition and dislocation mobility in sapphire. *J. Am. Ceram. Soc.*, 1994, **77**, 3099–3104.
27. Ochiai, S., Ikeda, S., Iwamoto, S., Sha, J., Okuda, H., Waku, Y. *et al.*, Residual stresses in YAG of melt growth Al2O3/YAG eutectic composite estimated by indentation fracture test and finite element analysis. In *Second Directionally Solidified Eutectic Ceramics International Workshop*, 2006.